Supplementary Information for:

In vitro and *in silico* analyses for predicting hepatic cytochrome P450-dependent metabolic potencies of polychlorinated biphenyls in the Baikal seal

Jean Yoo[†], Masashi Hirano[†], Hazuki Mizukawa[†§], Kei Nomiyama[†], Tetsuro Agusa[†], Eun-Young Kim[‡], Shinsuke Tanabe[†], and Hisato Iwata[†*]

†Center for Marine Environmental Studies (CMES), Ehime University, Bunkyo-cho 2-5, Matsuyama 790-8577, Japan

[‡]Department of Life and Nanopharmaceutical Science and Department of Biology, Kyung Hee University, Hoegi-Dong, Dongdaemun-Gu, Seoul 130-701, Korea

[§]Present address: Department of Environmental Veterinary Sciences,
Graduate School of Veterinary Medicine, Hokkaido University,
Kita 18, Nishi 9, Kita-ku, Sapporo 060-0818, Japan

[*]Corresponding author and address: Prof. Hisato Iwata
Center for Marine Environmental Studies (CMES), Ehime University
Bunkyo-cho 2-5, Matsuyama 790-8577, Japan
E-mail address: iwatah@agr.ehime-u.ac.jp

The supporting information contains 35 pages with 8 Tables and 10 Figures.

(access channel volume: 239 Å^3), (B) bsCYP1A2 (206 Å^3), (C) bsCYP1B1 (236 Å^3), (D) bsCYP2A (209 Å^3), (E) bsCYP2B (195 Å^3), and (F) bsCYP2C (437 Å^3). The access channel is colored in orange, and the heme is in black.

Page S34: **Figure S9.** Comparison of the distance from Cl-unsubstituted carbon of docked CB77 to the heme Fe in CYP1A1 homology models of 4 mammalian species. (A) Baikal seal, (B) Rat, (C) Guinea pig, and (D) Hamster. The heme, amino acid residues, and CB77 are shown in orange, grey, and pink, respectively. The shortest distance (Å) between Cl-unsubstituted carbon atom of CB77 and the heme Fe is shown in green line.

Page S35: **Figure S10.** Scatter plot of PC1 and PC4 obtained by PC analysis for all 62 PCB congeners examined. PCB congeners were divided into 2 groups (0–20% and >20%) based on the decreased ratio. PCB congeners with 0–20% and >20% decreased ratios are shown in white circles and red circles, respectively.

Materials and methods

Chemicals

The 62 PCB congeners used for the in vitro metabolism assay included CB1, CB3, CB4, CB8, CB10, CB15, CB18, CB19, CB22, CB28, CB33, CB37, CB44, CB49, CB52, CB54, CB70, CB74, CB77, CB81, CB87, CB95, CB99, CB101, CB104, CB105, CB110, CB114, CB118, CB119, CB123, CB126, CB128, CB138, CB149, CB151, CB153, CB155, CB156, CB157, CB158, CB167, CB168, CB169, CB170, CB171, CB177, CB178, CB180, CB183, CB187, CB188, CB189, CB191, CB194, CB199, CB201, CB202, CB205, CB206, CB208, and CB209. We selected these congeners based on their I-V structural properties, as categorized by Boon et al. (1997)[1], and the PCB congener profiles detected in the livers of Baikal seals[2]. Information on individual congeners is summarized in Table S1. These congeners were purchased from Wellington Laboratories Inc.

Sample collection

The liver tissues of Baikal seals were collected from Lake Baikal in 2005, as has been reported in our earlier studies.[3,4] Permission was granted by the Lake Baikal Basin Committee for Protection, Reproduction of Fish Resources and Fishing Control under the annual seal culling quota. The livers were removed on board immediately after animal collection, and the sub-samples were frozen and stored in liquid nitrogen until microsomal preparation.

Microsomal preparation and CYP spectral analysis

Liver microsomal fractions were prepared following the method of Guengerich (1982)[5]. About 6 g of liver tissue sample from one adult male Baikal seal (40.5 years old) was homogenized in five-fold volumes of cold homogenization buffer (50 M Tris-HCl, 0.15M KCl, pH 7.4–7.5) with a teflon-glass homogenizer (10 passes) and was centrifuged for 10 min at 750 × *g*. The supernatant was then centrifuged at 12,000 × *g* for 10 min. The supernatant was further centrifuged at 105,000 × *g* for 98 min. The supernatant (cytosol) fraction was removed, and the microsomal pellets were resuspended in one volume of TEDG buffer [50 mM Tris-HCl, 1 mM EDTA, 1 mM dithiothreitol, 20% (vol/vol) glycerol, pH 7.4–7.5]. Microsomal fractions were immediately frozen in liquid nitrogen, and stored at

-80°C until use.

Protein concentrations in microsomal fractions were determined by the bicinchoninic acid method.[6] BCA Protein Assay Reagent (Pierce, Rockford, IL) and bovine serum albumin as a standard were used for the protein assay. Absorbance at 560 nm was measured using a multiwell plate reader (SpectraFluor Plus, Tecan Austria GmbH, Groedig, Austria). The content of hepatic microsomal CYP was determined from the dithionite difference spectra of CO-treated samples[7] with a DU800 spectrophotometer (Beckman Coulter, Inc.).

Measurements of PCBs and OH-PCBs

The measurement of PCBs and OH-PCBs in the reaction mixture was performed according to the method of Nomiyama et al. (2010)[8]. Briefly, the reaction mixture was denatured with 6 M HCl and 2-propanol, and PCBs and OH-PCBs were extracted by 50% methyl t-butyl ether (MTBE)/hexane. The extract was partitioned into neutral and phenolic fractions using 1 M KOH in 50% ethanol/water. The neutral fraction containing PCBs was passed through a 4 g activated silica-gel column and eluted with 80 mL of 5% DCM/hexane.

The KOH solution containing OH-PCBs was acidified (pH 2) with sulfuric acid and was extracted twice with 50% MTBE/hexane. The organic fraction containing OH-PCBs was passed through a column packed with 3 g of hydrated silica gel (Wako-gel S-1, deactivated with 5% H_2O), and OH-PCBs was eluted with 50% dichloromethane (DCM)/hexane (100 mL). The eluted OH-PCB fraction was concentrated and dissolved in 1 mL hexane. The OH-PCBs were derivatized overnight by trimethylsilyldiazomethane. The derivatized (methylated) MeO-PCBs were passed through a 3 g activated silica-gel column, and were then eluted with 140 mL of 10% DCM/hexane. The PCBs and MeO-PCB fractions were concentrated to near dryness. Then, $^{13}C_{12}$-labeled PCBs dissolved in up to 50 μL of decane were injected as surrogates for the gas chromatograph (GC: 6890 series, Agilent) coupled with high resolution (>10,000) mass spectrometer (HRMS: MS-800D, JEOL) analysis. Identification and quantification of PCB congeners were performed under previously reported GC-HRMS analytical conditions.[8] Unknown OH-PCB metabolites were quantified as mean values of

relative response factors based on the identifiable $^{12}C_{12}$-OH-PCB homologues and the corresponding $^{13}C_{12}$-isomer in standard solution, following the method of Kunisue et al. (2007).[9]

Cloning and sequencing of bsCYP2 cDNAs

The cDNA of Baikal seal liver was prepared from poly(A)$^+$RNA using a Marathon cDNA Amplification Kit (BD Biosciences Clontech)[3]. Adaptors of adaptor primer 1 and 2 sequences were added to both ends of each cDNA. Partial cDNA sequences of bsCYP2A, 2B, and 2C were obtained from the cDNA library of the Baikal seal that was prepared for making the custom oligoarray[3]. To identify the full-length cDNA, primer sequences for RACE were designed based on the partial sequences (Table S2). The bsCYP2A primer for 5′-RACE was not designed because the 5′-sequence containing the start codon has already been obtained from the cDNA library. Amplification of the 5′- and 3′-ends of the cDNA was performed according to the protocol described in the Marathon™ Amplification Kit (Clontech Laboratories, Inc.). PCR reactions were as follows: 94°C for 30 sec, followed by 5 cycles of 94°C for 5 s and 72°C for 4 min, 5 cycles of 94°C for 5 s and 70°C for 4 min, and 25 cycles of 94°C for 5 s and 68°C for 4 min. BLAST homology searches in NCBI nucleotide sequence databases were applied to identify the bsCYP2 cDNAs based on high similarities to deposited sequences of other mammalian CYP2 genes. The molecular weight of bsCYP2 proteins was estimated using GENETYX-MAC version 14.0.11.

Multiple alignments of CYP2A, 2B, and 2C amino acid sequences were performed using the CLUSTAL_W in Mac Vector 11.1.1 program. The aligned amino acid sequences were used to construct a phylogenetic tree with the UPGMA and bootstrap (1000 samplings) method using Mac Vector.[10] Amino acid sequences of mammals except for the Baikal seal were obtained from the DNA Data Bank of Japan (DDBJ). The DDBJ accession numbers of mammalian CYPs used for constructing the phylogenetic tree are shown in Table S3.

***In silico* analysis**

All *in silico* analyses were carried out using the Molecular Operating Environment (MOE) program

(Chemical Computing Group, Montreal, Canada). For constructing homology models of the entire proteins of bsCYPs (1A1, 1A2, 1B1, 2A, 2B, and 2C), the following templates of CYP1 and 2 isoenzymes were taken from the Protein Data Bank (http://www.rcsb.org): human CYP1A1 (PDB code: 4I8V), human CYP1A2 (2HI4), human CYP1B1 (3PM0), human CYP2A6 (1Z10), rabbit CYP2B4 (1SUO), and human CYP2C9 (1OG5). All crystallographic water molecules were deleted from each template CYP structure. To adjust for structural defects and the clash of atoms, the Structure Preparation module in MOE was used. The amino acid sequences of bsCYPs and their template structures were aligned and carefully checked for conserved residual structure and gap positioning using the Protein Contacts program. In order to construct the 3D structure of heme-containing CYP proteins, a total of 500 generated structures (10 side chain samples per 50 main chain models) for each bsCYP were obtained by employing the 'induced fit' option that allows the heme iron to fit into the template structure. The 3D structures of bsCYPs were optimized by PFROSST force field[11] with an energy gradient of 0.05.[12] To generate the final model structure, the generalized Born/volume integral (GB/VI) model parameters[13] were applied. The overall geometric and stereochemical qualities of the homology models were assessed using Protein Geometry. Ramachandran plots of phi (φ) and psi (ψ) torsion angles for all of the residues and the clash of atoms in each model were checked and adjusted by energy minimization using the PFROSST force field.

Molecular docking simulations were performed to simulate the binding of 62 PCB congeners to bsCYP proteins using ASEDock (Ryoka Systems Inc., Tokyo, Japan) following the method of Goto et al. (2008).[14] Prior to the ASEDock analysis, structures of PCBs were constructed and energy minimized using Rebuild3D with MMFF94x force field in the MOE. A total of 500 confirmations for each PCB congener were generated using the default systematic search parameters by LowMode MD method. The parameters used for the refinement step were as follows: cutoff value of 4.5, RMS gradient of 10, and energy threshold of 500.[15] The energy of the PCB-CYP complex was refined using PFROSST of MOE under the limited conditions for which the side chains of amino acid residues were fixed. Each docking simulation was evaluated in terms of a U-dock score (kcal/mol): [U_ele (electric energy) + U_vdw (Van der Waals energy) + U_solv (solvation energy) + U_strain (strain energy)].

182 The distance between the Cl-unsubstituted carbon in a given PCB congener and the heme Fe in each
183 CYP was measured. The substrate binding pocket in each CYP was designed using Atom Region in
184 MOE.
185 Since the structure of substrate access channel may be a critical factor to affect the substrate
186 specificity of each CYP, we attempted to identify the access channel 2c, which is the most probable
187 candidate channel for substrates,[16] in each bsCYP protein, and compare their conformational
188 characteristics. By reference to the access channel 2c in human CYP2C9 model (PDB code: 1OG2)
189 reported in Otyepka et al. (2012),[16] the dummy sites in CYP2C9, which were selected by MOE, were
190 edited to fit the shape of channel 2c, and the channel was determined by using Atom Region in MOE.
191 The amino acid residues lining the access channel in CYP2C9 were identified, and the corresponding
192 amino acids in each bsCYP were assigned by aligning the bsCYP sequence with CYP2C9 sequence.
193 The structure of the channel 2c in each bsCYP, the cavity surrounded by the assigned amino acids,
194 was predicted by using Atom Region in MOE, and the volume was then measured.
195
196 **Statistical analyses**
197 All statistical analyses were conducted using the IBM SPSS Statistics 22.0 (IBM Corp., Armonk,
198 NY). Statistical significance was set at $p < 0.05$. Prior to PC analysis, Spearman's rank correlation test
199 was performed to examine correlations between decreased PCB ratios obtained in *in vitro* metabolism
200 assays and 119 factors (Table S4), which included structural and physicochemical parameters of PCB
201 congeners and *in silico* docking variables. Using these variables, PC analysis with VARIMAX
202 rotation was conducted.
203
204

References

1. Boon, J.P.; Meer, J.V.D.; Allchin, C.R.; Law, R.J.; Klungsøyr, J.; Leonards, P.E.G.; Spliid, H.; Storr-Hansen, E.; Mckenzie, C.; Wells, D.E. Concentration-dependent changes of PCB patterns in fish-eating mammals: structure evidence for induction of cytochrome P450. *Arch. Environ. Contam. Toxicol.* **1997**. 33 (3), 298-311.
2. Nomiyama, K.; Hirakawa, S.; Eguchi, A.; Kanbara, C.; Imaeda, D.; Yoo, J.; Kunisue, T.; Kim, E.; Iwata, H.; Tanabe, S. Toxicological assessment of polychlorinated biphenyls and their metabolites in the liver of Baikal seal (*Pusa sibirica*). *Environ. Sci. Technol.* **2014**. 48 (22), 13530–13539.
3. Hirakawa, S.; Imaeda, D.; Nakayama, K.; Udaka, M.; Kim, E.Y.; Kunisue, T.; Ogawa, M.; Matsuda, T.; Matsui, S.; Petrov, E.A.; Batoev, V.B.; Tanabe, S.; Iwata, H. Integrative assessment of potential effects of dioxins and related compounds in wild Baikal seals (*Pusa sibirica*): Application of microarray and biochemical analyses. *Aquat. Toxicol*. **2011**. 105 (1-2), 89–99.
4. Imaeda, D.; Nomiyama, K.; Kunisue, T.; Iwata, H.; Tsydenova, O.; Amano, M.; Petrov, E.A.; Batoev, B.V.; Tanabe, S. Blood levels of polychlorinated biphenyls and their hydroxylated metabolites in Baikal seals (*Pusa sibirica*): emphasis on interspecies comparison, gender difference and association with blood thyroid hormone levels. *Chemosphere*. **2014**. 144, 1-8.
5. Guengerich, F.P.; Dannan, G.A.; Wright, S.T.; Martin, M.V.; Kaminsky, L.S. Purification and characterization of liver microsomal cytochromes P-450: electrophoretic, spectral, catalytic, and immunochemical properties and inducibility of eight isozymes isolated from rats treated with phenobarbital or beta-naphthoflavone. *Biochemistry*. **1982**. 21 (23), 6019–6030.
6. Smith, P.K.; Krohn, R.I.; Hermanson, G.T.; Mallia, A.K.; Gartner, F.H.; Provenvzano, M.D.; Fujimoto, E.K.; Goeke, N.M.; Olson, B.J.; Klenk, D.C. Measurement of protein using bicinchoninic acid. *Anal. Biochem*. **1985**. 150 (1), 76–85.
7. Omura, T.; Sato, R. The carbon monoxide-binding pigment of liver microsomes: I. evidence for its hemoprotein nature. *J. Biol. Chem*. **1964**. 239, 2370-2378.
8. Nomiyama, K.; Murata, S.; Kunisue, T.; Yamada, T.K.; Mizukawa, H.; Takahashi, S.; Tanabe, S. Polychlorinated biphenyls and their hydroxylated metabolites (OH-PCBs) in the blood of toothed and baleen whales stranded along Japanese coastal waters. *Environ. Sci. Technol*. **2010**. 44 (10), 3732–3738.

9. Kunisue, T.; Sakiyama, T.; Yamada, T.K.; Takahashi, S.; Tanabe, S. Occurrence of hydroxylated polychlorinated biphenyls in the brain of cetaceans stranded along the Japanese coast. *Mar. Pollut. Bull*. **2007**. 54 (7), 963–973.
10. Lee, J.S.; Kim, E.Y.; Nomaru, K.; Iwata, H. Molecular and functional characterization of aryl hydrocarbon receptor repressor from the chicken (*Gallus gallus*): interspecies similarities and differences. *Toxicol. Sci*. **2011**. 119 (2), 319-334.
11. Amari, S.; Kataoka, R.; Ikegami, T.; Hirayama, N. HLA-Modeler: automated homology modeling of human leukocyte antigens. *Int. J. Med. Chem*. **2013**. Article ID. 690513. 6 pages
12. Wang, J.; Cieplak, P.; Kollman, P.A. How well does a restrained electrostatic potential (RESP) model perform in calculating conformational energies of organic and biological molecules? *J. Comput. Chem*. **2000**. 21 (12), 1049–1074.
13. Labute, P. The generalized Born/volume integral implicit solvent model: Estimation of the free energy of hydration using London dispersion instead of atomic surface area. *J. Comput. Chem*. **2008**. 29 (10), 1693-1698.
14. Goto, J.; Kataoka, R.; Muta, Hajime.; Hirayama, N. ASEDock-Docking Based on Alpha Spheres and Excluded Volumes. *J. Chem. Inf. Model*. **2008**. 48 (3), 583–590.
15. Labute, P. LowModeMD--implicit low-mode velocity filtering applied to conformational search of macrocycles and protein loops. *J. Chem. Inf. Model*. **2010**. 50 (5), 792-800.
16. Otyepka, M.; Berka, K.; Anzenbacher, P. Is there a relationship between the substrate preferences and structural flexibility of cytochromes P450? *Curr. Drug Metab*. **2012**. 13 (2), 130-142.

Table S1. IUPAC numbers and structural characteristics of 62 PCB congeners used in *in vitro* metabolism assay.

IUPAC no.	Cl no.	IUPAC name	No. pairs *o, m*-vic. H-atoms	No. pairs *m, p*- vic. H-atoms	No. *o*-Cl atoms	Metabolic group[a]
1	1	2-Chlorobiphenyl	3	4	1	Ⅲ, Ⅳ
3	1	4-Chlorobiphenyl	4	2	0	Ⅲ, Ⅳ
4	2	2,2'-Dichlorobiphenyl	2	4	2	Ⅱ, Ⅳ
8	2	2,4'-Dichlorobiphenyl	3	2	1	Ⅲ, Ⅳ
10	2	2,6-Dichlorobiphenyl	2	4	2	Ⅱ, Ⅳ
15	2	4,4'-Dichlorobiphenyl	4	0	0	Ⅲ
18	3	2,2',5-Trichlorobiphenyl	1	3	2	Ⅱ, Ⅳ
19	3	2,2',6-Trichlorobiphenyl	1	4	3	Ⅱ, Ⅴ
22	3	2,3,4'-Trichlorobiphenyl	3	1	1	Ⅲ, Ⅳ
28	3	2,4,4'-Trichlorobiphenyl	3	0	1	Ⅲ
33	3	2,3',4'-Trichlorobiphenyl	2	2	1	Ⅲ, Ⅳ
37	3	3,4,4'-Trichlorobiphenyl	3	0	0	Ⅲ
44	4	2,2',3,5'-Tetrachlorobiphenyl	1	2	2	Ⅱ, Ⅳ
49	4	2,2',4,5'-Tetrachlorobiphenyl	1	1	2	Ⅱ, Ⅳ
52	4	2,2',5,5'-Tetrachlorobiphenyl	0	2	2	Ⅳ
54	4	2,2',6,6'-Tetrachlorobiphenyl	0	4	4	Ⅳ
70	4	2,3',4',5-Tetrachlorobiphenyl	1	1	1	Ⅲ, Ⅳ
74	4	2,4,4',5-Tetrachlorobiphenyl	2	0	1	Ⅲ
77	4	3,3',4,4'-Tetrachlorobiphenyl	2	0	0	Ⅲ
81	4	3,4,4',5-Tetrachlorobiphenyl	2	0	0	Ⅲ
87	5	2,2',3,4,5'-Pentachlorobiphenyl	1	1	2	Ⅱ, Ⅳ
95	5	2,2',3,5',6-Pentachlorobiphenyl	0	2	3	Ⅴ
99	5	2,2',4,4',5-Pentachlorobiphenyl	1	0	2	Ⅱ
101	5	2,2',4,5,5'-Pentachlorobiphenyl	0	1	2	Ⅳ
104	5	2,2',4,6,6'-Pentachlorobiphenyl	0	2	4	Ⅴ
105	5	2,3,3',4,4'-Pentachlorobiphenyl	2	0	1	Ⅲ
110	5	2,3,3',4',6-Pentachlorobiphenyl	1	1	2	Ⅱ, Ⅳ
114	5	2,3,4,4',5-Pentachlorobiphenyl	2	0	1	Ⅲ
118	5	2,3',4,4',5-Pentachlorobiphenyl	1	0	1	Ⅲ
119	5	2,3',4,4',6-Pentachlorobiphenyl	1	0	2	Ⅱ
123	5	2,3',4,4',5'-Pentachlorobiphenyl	1	0	1	Ⅲ
126	5	3,3',4,4',5-Pentachlorobiphenyl	1	0	0	Ⅲ
128	6	2,2',3,3',4,4'-Hexachlorobiphenyl	2	0	2	Ⅱ
138	6	2,2',3,4,4',5'-Hexachlorobiphenyl	1	0	2	Ⅱ
149	6	2,2',3,4',5',6-Hexachlorobiphenyl	0	1	3	Ⅴ
151	6	2,2',3,5,5',6-Hexachlorobiphenyl	0	1	3	Ⅴ
153	6	2,2',4,4',5,5'-Hexachlorobiphenyl	0	0	2	Ⅰ
155	6	2,2',4,4',6,6'-Hexachlorobiphenyl	0	0	4	Ⅰ
156	6	2,3,3',4,4',5-Hexachlorobiphenyl	1	0	1	Ⅲ
157	6	2,3,3',4,4',5'-Hexachlorobiphenyl	1	0	1	Ⅲ

158	6	2,3,3',4,4',6-Hexachlorobiphenyl	1	0	2	II
167	6	2,3',4,4',5,5'-Hexachlorobiphenyl	0	0	1	I
168	6	2,3',4,4',5',6-Hexachlorobiphenyl	0	0	2	I
169	6	3,3',4,4',5,5'-Hexachlorobiphenyl	0	0	0	I
170	7	2,2',3,3',4,4',5-Heptachlorobiphenyl	1	0	2	II
171	7	2,2',3,3',4,4',6-Heptachlorobiphenyl	1	0	3	II
177	7	2,2',3,3',4,5',6'-Heptachlorobiphenyl	1	0	3	II
178	7	2,2',3,3',5,5',6-Heptachlorobiphenyl	0	0	3	I
180	7	2,2',3,4,4',5,5'-Heptachlorobiphenyl	0	0	2	I
183	7	2,2',3,4,4',5',6-Heptachlorobiphenyl	0	0	3	I
187	7	2,2',3,4',5,5',6-Heptachlorobiphenyl	0	0	3	I
188	7	2,2',3,4',5,6,6'-Heptachlorobiphenyl	0	0	4	I
189	7	2,3,3',4,4',5,5'-Heptachlorobiphenyl	0	0	1	I
191	7	2,3,3',4,4',5',6-Heptachlorobiphenyl	0	0	2	I
194	8	2,2',3,3',4,4',5,5'-Octachlorobiphenyl	0	0	2	I
199	8	2,2',3,3',4,5,5',6'-Octachlorobiphenyl	0	0	3	I
201	8	2,2',3,3',4,5',6,6'-Octachlorobiphenyl	0	1	4	V
202	8	2,2',3,3',5,5',6,6'-Octachlorobiphenyl	0	0	4	I
205	8	2,3,3',4,4',5,5',6-Octachlorobiphenyl	0	0	2	I
206	9	2,2',3,3',4,4',5,5',6-Nonachlorobiphenyl	0	0	3	I
208	9	2,2',3,3',4,5,5',6,6'-Nonachlorobiphenyl	0	0	4	I
209	10	Decachlorobiphenyl	0	0	4	I

[a] Classification of PCB congeners based on the predicted potency of CYP-mediated metabolism proposed by Boon et al. (1997) as follows;

I: Congeners without any vicinal hydrogen (H)-atoms (persistent)

II: Congeners with vicinal H-atoms exclusively in the *ortho*- and *meta*-positions in combination with ≥2 *ortho*-Cl substituents (persistent)

III: Congeners with vicinal H-atoms in the *ortho*- and *meta*-positions in combination with ≤1 *ortho*-Cl (metabolizable at a constant rate or by inducible CYP isozymes)

IV: Congeners with vicinal H-atoms in the *meta*- and *para*-positions in combination with ≤2 *ortho*-Cl (metabolizable at a constant rate or by inducible CYP isozymes)

V: Congeners with vicinal H-atoms in the *meta*- and *para*-positions in combination with ≥3 *ortho*-Cl (metabolizable at a constant rate or by inducible CYP isozymes)

Table S2. Primer sequences used for the RACE of bsCYP2 cDNAs.

Primer name	Sequence
bsCYP2A 3'-RACE	5'-CCAGCACTTCCTGGATGAGAATGGGCAG-3'
bsCYP2B 5'-RACE	5'-AGCCGCAGCAATTCAGGGTCTCTGTAGC-3
bsCYP2B 3'-RACE	5'-CTAGCTTCAGAGGGTACATCATTCCCA-3
bsCYP2C 5'-RACE	5'-CTAAGCAAGCTAGCAGCAGAGAAT-3'
bsCYP2C 3'-RACE	5’-GCAAGACAGGAGCCGCATGCCCTACACG-3’

Table S3. Accession numbers of mammalian CYP2 sequences used for constructing the phylogenic tree shown in Figure S5.

CYP	accession number
CYP2A	dog CYP2A13 (DQ238561), dog CYP2A25 (DQ238562), horse CYP2A13 (EU286274), human CYP2A6 (AF182275), human CYP2A13 (AY513606), monkey CYP2A23 (DQ074790), mouse CYP2A5 (P20852), mouse CYP2A4 (Q91X75), rat CYP2A1 (P11711), rat CYP2A2 (P15149), rat CYP2A3 (P20812), pig CYP2A19 (AB052255), rabbit CYP2A11 (Q05556), rabbit CYP2A10 (Q05555)
CYP2B	rat CYP2B1 (P00176), rat CYP2B2 (P04167), rat CYP2B3 (P13107), cattle CYP2B6 (no accession no.), dog CYP2B11 (P24460), monkey CYP2B6 (DQ074793), monkey CYP2B30 (AY635461), human CYP2B6 (P20813), human CYP2B7 (DQ198366), mouse CYP2B9 (P12790), mouse CYP2B10 (P12791), mouse CYP2B13 (A6H6J2), mouse CYP2B19 (O55071), mouse CYP2B23 (no accession no.), rabbit CYP2B4 (P00178), pig CYP2B22 (AB052256)
CYP2C	dog CYP2C21 (P56594), dog CYP2C41 (AF016248), horse CYP2C92 (EU014893), human CYP2C8 (P10632), human CYP2C9 (P11712), human CYP2C19 (P33261), monkey CYP2C18 (DQ297681), minke whale CYP2C78 (AB290008), mouse CYP2C29 (Q64458), rabbit CYP2C1 (P00180), rabbit CYP2C2 (P00181), rat CYP2C6 (P05178), rat CYP2C7 (Q4QQW7), pig CYP2C33 (AB052257), pig CYP2C49 (AB052258)
CYP3A	human CYP3A4 (P08684)

The human CYP3A4 is used as an outlier.

280 Table S4. Parameters used for principle component analysis.

Group	Parameter
In vitro PCB metabolism assay	PCB decrease ratio%
PCB structural parameters	number of Cl in PCB
	presence of non-*ortho*-position
	presence of mono-*ortho*-position
	number of H atom at *ortho*-position
	number of H atom at *meta*-position
	number of H atom at *para*-position
	number of sites with vicinal H atoms at *ortho*- and *meta*-positions of PCB
	number of sites with vicinal H atoms at *meta*- and *para*-positions of PCB
	number of Cl at *ortho*-position
	number of Cl at *meta*-position
	number of Cl at para-position
	number of H at ∑(*ortho*+*meta*)
	number of H at ∑(*para*+*meta*)
	presence of vicinal H atoms at 2 and 3 position of PCB
	presence of vicinal H atoms at 2' and 3' position of PCB
	presence of vicinal H atoms at 3 and 4 position of PCB
	presence of vicinal H atoms at 3' and 4' position of PCB
	presence of vicinal H atoms at 4 and 5 position of PCB
	presence of vicinal H atoms at 4' and 5' position of PCB
	presence of vicinal H atoms at 5 and 6 position of PCB
	presence of vicinal H atoms at 5' and 6' position of PCB
	bilateral symmetry
Physicochemical parameters	Log Kow
	molecular weight ofPCB
	PEOE_VSA+0_(electricity effect)
	PEOE_VSA+1_(electricity effect)
	PEOE_VSA-1_(electricity effect)
	SlogP_VSA6_(hydrophobicity)
	SlogP_VSA7_(hydrophobicity)
	SlogP_VSA9_(hydrophobicity)
	SMR_VSA3_(molar refractivity)
	SMR_VSA5_(molar refractivity)
	SMR_VSA7_(molar refractivity)

281 (continued)

282

Group	Parameter
In silico results	U_dock value of the interaction of PCB with bsCYP1A1
	presence of measurable distance from bsCYP1A1 heme Fe to Cl-unsubstituted carbon at 2 position of PCB
	presence of measurable distance from bsCYP1A1 heme Fe to Cl-unsubstituted carbon at 2' position of PCB
	presence of measurable distance from bsCYP1A1 heme Fe to Cl-unsubstituted carbon at 3 position of PCB
	presence of measurable distance from bsCYP1A1 heme Fe to Cl-unsubstituted carbon at 3' position of PCB
	presence of measurable distance from bsCYP1A1 heme Fe to Cl-unsubstituted carbon at 4 position of PCB
	presence of measurable distance from bsCYP1A1 heme Fe to Cl-unsubstituted carbon at 4' position of PCB
	presence of measurable distance from bsCYP1A1 heme Fe to Cl-unsubstituted carbon at 5 position of PCB
	presence of measurable distance from bsCYP1A1 heme Fe to Cl-unsubstituted carbon at 5' position of PCB
	presence of measurable distance from bsCYP1A1 heme Fe to Cl-unsubstituted carbon at 6 position of PCB
	presence of measurable distance from bsCYP1A1 heme Fe to Cl-unsubstituted carbon at 6' position of PCB
	shortest measurable distance(Å) from bsCYP1A1 heme Fe to Cl-unsubstituted carbons of PCB
	ranking number of docking simulation in bsCYP1A1
	number of posing of docked PCBs of which Cl-unsubstituted carbon was allocated within 5Å distance from the heme Fe in bsCYP1A1
	number of posing of docked PCBs of which Cl-unsubstituted carbon was allocated within 6Å distance from the heme Fe in bsCYP1A1
	U_dock value of the interaction of PCB with bsCYP1A2
	presence of measurable distance from bsCYP1A2 heme Fe to Cl-unsubstituted carbon at 2 position of PCB
	presence of measurable distance from bsCYP1A2 heme Fe to Cl-unsubstituted carbon at 2' position of PCB
	presence of measurable distance from bsCYP1A2 heme Fe to Cl-unsubstituted carbon at 3 position of PCB
	presence of measurable distance from bsCYP1A2 heme Fe to Cl-unsubstituted carbon at 3' position of PCB
	presence of measurable distance from bsCYP1A2 heme Fe to Cl-unsubstituted carbon at 4 position of PCB
	presence of measurable distance from bsCYP1A2 heme Fe to Cl-unsubstituted carbon at 4' position of PCB
	presence of measurable distance from bsCYP1A2 heme Fe to Cl-unsubstituted carbon at 5 position of PCB
	presence of measurable distance from bsCYP1A2 heme Fe to Cl-unsubstituted carbon at 5' position of PCB
	presence of measurable distance from bsCYP1A2 heme Fe to Cl-unsubstituted carbon at 6 position of PCB
	presence of measurable distance from bsCYP1A2 heme Fe to Cl-unsubstituted carbon at 6' position of PCB
	shortest measurable distance(Å) from bsCYP1A2 heme Fe to Cl-unsubstituted carbons of PCB
	ranking number of docking simulation in bsCYP1A2
	number of posing of docked PCBs of which Cl-unsubstituted carbon was allocated within 5Å distance from the heme Fe in bsCYP1A2
	number of posing of docked PCBs of which Cl-unsubstituted carbon was allocated within 6Å distance from the heme Fe in bsCYP1A2
	U_dock value of the interaction of PCB with bsCYP1B1
	presence of measurable distance from bsCYP1B1 heme Fe to Cl-unsubstituted carbon at 2 position of PCB
	presence of measurable distance from bsCYP1B1 heme Fe to Cl-unsubstituted carbon at 2' position of PCB
	presence of measurable distance from bsCYP1B1 heme Fe to Cl-unsubstituted carbon at 3 position of PCB

(continued)

Group	Parameter
In silico results	presence of measurable distance from bsCYP1B1 heme Fe to Cl-unsubstituted carbon at 3' position of PCB
	presence of measurable distance from bsCYP1B1 heme Fe to Cl-unsubstituted carbon at 4 position of PCB
	presence of measurable distance from bsCYP1B1 heme Fe to Cl-unsubstituted carbon at 4' position of PCB
	presence of measurable distance from bsCYP1B1 heme Fe to Cl-unsubstituted carbon at 5 position of PCB
	presence of measurable distance from bsCYP1B1 heme Fe to Cl-unsubstituted carbon at 5' position of PCB
	presence of measurable distance from bsCYP1B1 heme Fe to Cl-unsubstituted carbon at 6 position of PCB
	presence of measurable distance from bsCYP1B1 heme Fe to Cl-unsubstituted carbon at 6' position of PCB
	shortest measurable distance(Å) from bsCYP1B1 heme Fe to Cl-unsubstituted carbons of PCB
	ranking number of docking simulation in bsCYP1B1
	number of posing of docked PCBs of which Cl-unsubstituted carbon was allocated within 5Å distance from the heme Fe in bsCYP1B1
	number of posing of docked PCBs of which Cl-unsubstituted carbon was allocated within 6Å distance from the heme Fe in bsCYP1B1
	U_dock value of the interaction of PCB with bsCYP2A
	presence of measurable distance from bsCYP2A heme Fe to Cl-unsubstituted carbon at 2 position of PCB
	presence of measurable distance from bsCYP2A heme Fe to Cl-unsubstituted carbon at 2' position of PCB
	presence of measurable distance from bsCYP2A heme Fe to Cl-unsubstituted carbon at 3 position of PCB
	presence of measurable distance from bsCYP2A heme Fe to Cl-unsubstituted carbon at 3' position of PCB
	presence of measurable distance from bsCYP2A heme Fe to Cl-unsubstituted carbon at 4 position of PCB
	presence of measurable distance from bsCYP2A heme Fe to Cl-unsubstituted carbon at 4' position of PCB
	presence of measurable distance from bsCYP2A heme Fe to Cl-unsubstituted carbon at 5 position of PCB
	presence of measurable distance from bsCYP2A heme Fe to Cl-unsubstituted carbon at 5' position of PCB
	presence of measurable distance from bsCYP2A heme Fe to Cl-unsubstituted carbon at 6 position of PCB
	presence of measurable distance from bsCYP2A heme Fe to Cl-unsubstituted carbon at 6' position of PCB
	shortest measurable distance(Å) from bsCYP2A heme Fe to Cl-unsubstituted carbons of PCB
	ranking number of docking simulation in bsCYP2A
	number of posing of docked PCBs of which Cl-unsubstituted carbon was allocated within 5Å distance from the heme Fe in bsCYP2A
	number of posing of docked PCBs of which Cl-unsubstituted carbon was allocated within 6Å distance from the heme Fe in bsCYP2A
	U_dock value of the interaction of PCB with bsCYP2B
	presence of measurable distance from bsCYP2B heme Fe to Cl-unsubstituted carbon at 2 position of PCB
	presence of measurable distance from bsCYP2B heme Fe to Cl-unsubstituted carbon at 2' position of PCB
	presence of measurable distance from bsCYP2B heme Fe to Cl-unsubstituted carbon at 3 position of PCB
	presence of measurable distance from bsCYP2B heme Fe to Cl-unsubstituted carbon at 3' position of PCB
	presence of measurable distance from bsCYP2B heme Fe to Cl-unsubstituted carbon at 4 position of PCB
	presence of measurable distance from bsCYP2B heme Fe to Cl-unsubstituted carbon at 4' position of PCB

(continued)

Group	Parameter
In silico results	presence of measurable distance from bsCYP2B heme Fe to Cl-unsubstituted carbon at 5 position of PCB
	presence of measurable distance from bsCYP2B heme Fe to Cl-unsubstituted carbon at 5' position of PCB
	presence of measurable distance from bsCYP2B heme Fe to Cl-unsubstituted carbon at 6 position of PCB
	presence of measurable distance from bsCYP2B heme Fe to Cl-unsubstituted carbon at 6' position of PCB
	shortest measurable distance(Å) from bsCYP2B heme Fe to Cl-unsubstituted carbons of PCB
	ranking number of docking simulation in bsCYP2B
	number of posing of docked PCBs of which Cl-unsubstituted carbon was allocated within 5Å distance from the heme Fe in bsCYP2B
	number of posing of docked PCBs of which Cl-unsubstituted carbon was allocated within 6Å distance from the heme Fe in bsCYP2B
	U_dock value of the interaction of PCB with bsCYP2C
	presence of measurable distance from bsCYP2C heme Fe to Cl-unsubstituted carbon at 2 position of PCB
	presence of measurable distance from bsCYP2C heme Fe to Cl-unsubstituted carbon at 2' position of PCB
	presence of measurable distance from bsCYP2C heme Fe to Cl-unsubstituted carbon at 3 position of PCB
	presence of measurable distance from bsCYP2C heme Fe to Cl-unsubstituted carbon at 3' position of PCB
	presence of measurable distance from bsCYP2C heme Fe to Cl-unsubstituted carbon at 4 position of PCB
	presence of measurable distance from bsCYP2C heme Fe to Cl-unsubstituted carbon at 4' position of PCB
	presence of measurable distance from bsCYP2C heme Fe to Cl-unsubstituted carbon at 5 position of PCB
	presence of measurable distance from bsCYP2C heme Fe to Cl-unsubstituted carbon at 5' position of PCB
	presence of measurable distance from bsCYP2C heme Fe to Cl-unsubstituted carbon at 6 position of PCB
	presence of measurable distance from bsCYP2C heme Fe to Cl-unsubstituted carbon at 6' position of PCB
	shortest measurable distance(Å) from bsCYP2C heme Fe to Cl-unsubstituted carbons of PCB
	ranking number of docking simulation in bsCYP2C
	number of posing of docked PCBs of which Cl-unsubstituted carbon was allocated within 5Å distance from the heme Fe in bsCYP2C
	number of posing of docked PCBs of which Cl-unsubstituted carbon was allocated within 6Å distance from the heme Fe in bsCYP2C

289 Table S5. Validation of the homology models of bsCYP1A1, 1A2, 1B1, 2A, 2B, and 2C.

CYP isozyme	PCB congener	Distance (Å) between Cl unsubstituted carbon of PCB and the heme Fe in the top 3 CYP models		
		average	std	cv %
bsCYP1A1	CB180	8.1	0.1	0.6
	CB199	7.6	5.0	65.3
	CB209	5.1	1.2	23.5
bsCYP1A2	CB15	7.0	1.2	17.2
	CB44	5.1	0.6	11.6
	CB110	5.8	1.5	25.4
bsCYP1B1	CB52	6.2	0.8	12.7
	CB183	5.7	1.8	32.1
	CB206	8.9	1.8	20.6
bsCYP2A	CB19	4.1	0.6	14.7
	CB70	3.6	0.8	20.9
	CB205	5.7	0.7	11.6
bsCYP2B	CB3	2.8	0.3	9.5
	CB74	3.6	0.3	7.9
	CB206	6.1	1.0	16.1
bsCYP2C	CB37	9.3	2.5	26.5
	CB44	9.3	0.6	6.9
	CB191	9.8	0.5	5.2

290

291 Top 3 homology models of each CYP with the 1st, 2nd, and 3rd lowest total potential energies were
292 constructed, and validated by the variation (average, standard variation (std) and CV%) in the distance
293 between Cl unsubstituted carbon of some PCB congeners and the heme Fe in the top 3 CYP models.
294 For the validation of the top 3 models for each bsCYP isozyme, we applied 3 PCB congeners which
295 showed the shortest, longest, and median distance between Cl unsubstituted carbon of the PCB and
296 the heme in the 1st ranked model.

297

298 Table S6. Estimated shortest distance (Å) between Cl-unsubstituted carbon of each PCB congener and

299 the heme Fe in bsCYP1 and bsCYP2 protein homology models.

IUPAC No.	CYP1A1	CYP1A2	CYP1B1	CYP2A	CYP2B	CYP2C
1	8.98	4.95	4.75	5.80	3.94	8.15
3	8.11	6.14	7.33	4.92	3.08	9.64
4	7.99	4.34	4.01	4.21	3.55	7.81
8	8.90	6.27	5.31	4.31	3.26	7.06
10	7.99	4.34	4.01	4.21	3.55	7.81
15	8.00	8.43	4.88	2.98	3.13	10.16
18	7.69	7.47	5.35	4.87	4.81	9.69
19	8.07	4.60	4.23	4.70	3.38	9.21
22	7.75	5.14	4.16	3.30	3.55	8.33
28	11.04	6.46	5.99	4.45	3.68	8.06
33	7.39	5.64	5.26	3.89	4.15	8.66
37	8.69	4.74	5.67	3.72	3.17	6.62
44	6.78	5.75	5.62	4.79	4.30	9.50
49	7.39	4.27	4.42	3.27	3.47	7.60
52	7.85	5.37	5.48	4.40	3.65	9.77
54	9.19	5.19	4.16	3.92	3.46	9.60
70	8.23	5.07	4.58	2.73	3.37	10.27
74	8.28	6.26	5.67	4.70	3.80	10.03
77	7.88	5.75	5.88	3.62	3.77	7.68
81	8.05	5.94	5.86	4.21	4.02	8.29
87	8.93	6.27	5.82	5.09	4.37	8.25
95	8.37	6.33	10.70	4.57	3.79	9.99
99	8.43	4.51	4.67	3.13	3.39	8.36
101	8.23	5.34	4.56	4.96	3.90	8.78
104	8.01	4.91	4.13	3.71	3.66	8.18
105	8.29	4.62	4.42	4.25	4.23	9.59
110	6.89	4.14	6.75	4.78	4.10	9.01
114	8.04	6.33	6.65	4.76	3.60	7.98
118	7.77	6.39	5.79	5.36	3.70	9.93
119	7.06	5.95	6.03	4.39	4.00	7.76
123	8.03	4.60	6.74	4.67	3.72	8.25
126	8.86	6.03	4.93	4.99	4.12	8.96
128	9.04	6.29	5.90	4.08	4.18	8.26
138	7.86	4.15	4.00	5.18	3.37	8.22
149	7.04	5.78	7.78	4.47	4.10	8.33
151	9.07	5.17	5.41	3.83	3.79	10.20
153	8.48	5.04	4.98	4.75	3.99	8.65
155	8.08	5.50	4.72	4.12	4.23	9.70
156	8.81	6.44	8.54	5.43	5.55	8.43
157	7.67	6.39	7.82	4.63	5.08	8.71
158	7.19	6.03	6.99	4.68	4.15	8.29
167	8.02	5.22	5.39	4.85	4.90	9.03
168	8.98	6.44	4.77	5.74	3.63	9.26
169	9.81	6.41	6.98	5.69	5.63	8.74
170	9.05	4.40	5.91	5.49	4.98	8.44
171	7.85	7.35	4.23	5.14	4.63	9.35
177	8.22	6.54	5.88	4.67	3.76	9.08
178	8.37	5.06	9.32	3.59	4.88	8.71
180	8.14	6.10	4.56	5.67	3.12	8.47
183	8.36	4.68	3.86	4.27	3.73	10.25
187	8.73	6.14	5.66	4.77	3.53	8.92
188	8.75	6.39	5.45	4.72	3.17	9.76
189	9.63	6.57	6.58	5.35	5.64	8.52
191	7.04	4.69	5.20	5.77	3.43	10.40
194	8.84	5.39	9.12	5.04	5.78	9.56
199	13.04	6.06	5.25	4.42	5.31	8.25
201	7.14	6.65	8.15	4.75	3.74	9.55
202	8.10	5.35	4.69	3.33	6.11	9.78
205	10.85	7.93	10.39	6.42	5.72	10.11

206	10.89	5.26	10.86	4.85	6.38	8.39
208	7.80	6.65	5.95	4.75	3.77	8.02
209	6.10	4.85	4.23	4.83	3.92	9.19

300

301

302 Table S7. PC1-5 scores obtained by PC analysis for all of 62 PCB congeners examined.

Parameter	PC1	PC2	PC3	PC4	PC5
In vitro decreased ratio of PCB (%)	0.55	0.19	0.08	0.51	-0.01
Number of Cl in PCB	-0.95	-0.10	-0.16	-0.02	0.05
Molecular weight of PCB	-0.95	-0.10	-0.16	-0.02	0.05
Log Kow of PCB	-0.89	-0.20	-0.36	-0.02	0.12
Number of H atom at *meta*-position of PCB	0.85	0.18	0.18	-0.07	-0.16
Number of sites with vicinal H atoms at *meta*- and *para*-positions of PCB	0.75	0.29	0.50	-0.04	-0.19
Presence of vicinal H atoms at *meta*- and *para*-positions of PCB	0.50	0.11	0.80	-0.11	-0.03
Presence of Cl-substitution at 4' position of PCB	-0.01	-0.13	-0.80	-0.25	0.14
Presence of vicinal H atoms at 2 and 3 positions of PCB	0.45	-0.19	-0.07	0.59	0.08
Presence of vicinal H atoms at 5 and 6 positions of PCB	0.64	-0.08	-0.19	0.21	-0.12
Presence of vicinal H atoms at 4’ and 5’ positions of PCB	0.32	-0.07	0.82	0.16	-0.01
Presence of measurable distance from bsCYP1A1 heme Fe to Cl-unsubstituted carbon at 3' position of PCB	0.08	0.27	0.26	0.34	0.01
Presence of measurable distance from bsCYP1A2 heme Fe to Cl-unsubstituted carbon at 6 position of PCB	-0.15	-0.20	0.03	-0.07	0.69
Number of posing of docked PCBs of which Cl-unsubstituted carbon was allocated within 6 Å distance from the heme Fe in bsCYP1A2	0.01	0.63	0.16	-0.26	0.10
Presence of measurable distance from bsCYP1B1 heme Fe to Cl-unsubstituted carbon at 4’ position of PCB	0.04	0.27	0.05	0.67	-0.16
Presence of measurable distance from bsCYP1B1 heme Fe to Cl-unsubstituted carbon at 5 position of PCB	-0.09	0.06	-0.18	-0.11	0.74
Shortest measurable distance (Å) from bsCYP2A heme Fe to Cl-unsubstituted carbons of PCB	-0.28	-0.78	0.16	-0.29	0.11
Number of posing of docked PCBs of which Cl-unsubstituted carbon was allocated within 5 Å distance from the heme Fe in bsCYP2A	0.09	0.81	0.11	0.21	-0.21
Number of posing of docked PCBs of which Cl-unsubstituted carbon was allocated within 6 Å distance from the heme Fe in bsCYP2A	0.16	0.82	0.05	0.12	-0.05
Presence of measurable distance from bsCYP2B heme Fe to Cl-unsubstituted carbon at 4’ position of PCB	-0.14	0.01	0.19	0.78	-0.08
Presence of measurable distance from bsCYP2B heme Fe to Cl-unsubstituted carbon at 6 position of PCB	-0.14	-0.05	-0.02	0.02	0.89
U_dock value of the interaction of PCB with bsCYP2C (kcal/mol)	0.85	0.13	0.16	0.11	-0.14

303

304

305 Table S8. PC1-4 scores obtained by PC analysis for 1-5 chlorine substituted PCB congeners examined.

Parameter	PC1	PC2	PC3	PC4
In vitro decreased ratio of PCB (%)	-0.41	0.59	0.23	0.37
Number of Cl in PCB	0.94	-0.03	-0.20	-0.17
Molecular weight of PCB	0.94	-0.03	-0.20	-0.17
Log Kow of PCB	0.90	-0.08	0.00	-0.21
Number of H atom at *meta*-position of PCB	-0.75	0.28	0.00	0.18
Presence of Cl-substitution at 5 position of PCB	0.22	-0.13	-0.01	-0.92
Presence of vicinal H atoms at 2 and 3 positions of PCB	-0.41	0.19	0.64	0.05
Presence of vicinal H atoms at 5 and 6 positions of PCB	-0.43	-0.08	0.14	0.69
Number of posing of docked PCBs of which Cl-unsubstituted carbon was allocated within 6Å distance from the heme Fe in bsCYP1A2	0.13	0.40	-0.66	0.18
Shortest measurable distance (Å) from bsCYP1B1 heme Fe to Cl-unsubstituted carbons of PCB	0.43	-0.28	0.62	0.18
Shortest measurable distance (Å) from bsCYP2A heme Fe to Cl-unsubstituted carbons of PCB	0.03	-0.81	0.11	0.09
Number of posing of docked PCBs of which Cl-unsubstituted carbon was allocated within 6Å distance from the heme Fe in bsCYP2A	0.11	0.79	-0.09	0.14
Presence of measurable distance from bsCYP2B heme Fe to Cl-unsubstituted carbon at 4' position of PCB	-0.20	0.27	0.72	0.20
Shortest measurable distance (Å) from bsCYP2B heme Fe to Cl-unsubstituted carbons of PCB	0.35	-0.67	-0.33	0.10
U_dock value of the interaction of PCB with bsCYP2C (kcal/mol)	-0.88	-0.07	0.16	0.15

306

307

308

309

310

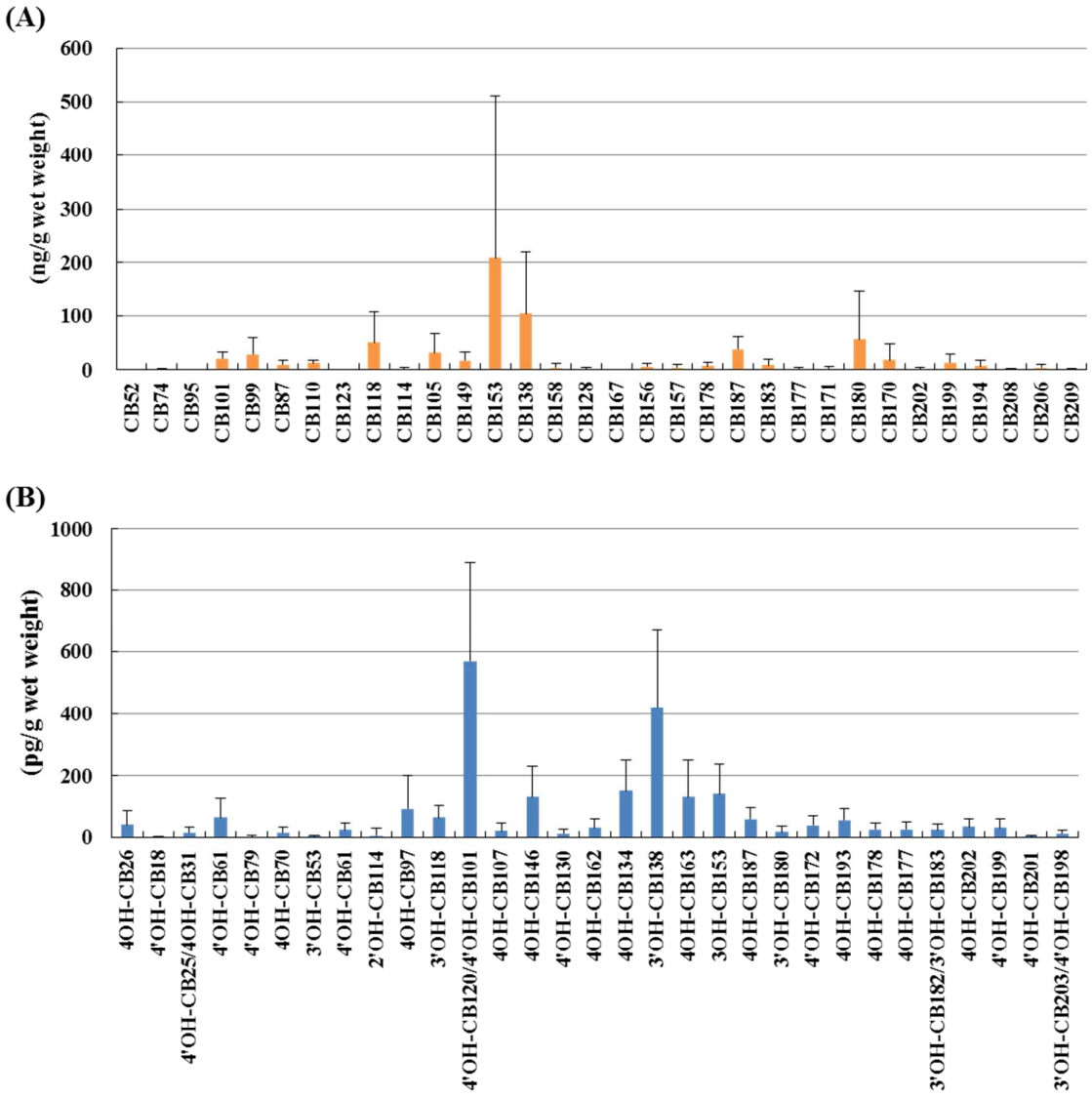

311

312 Figure S1.

313

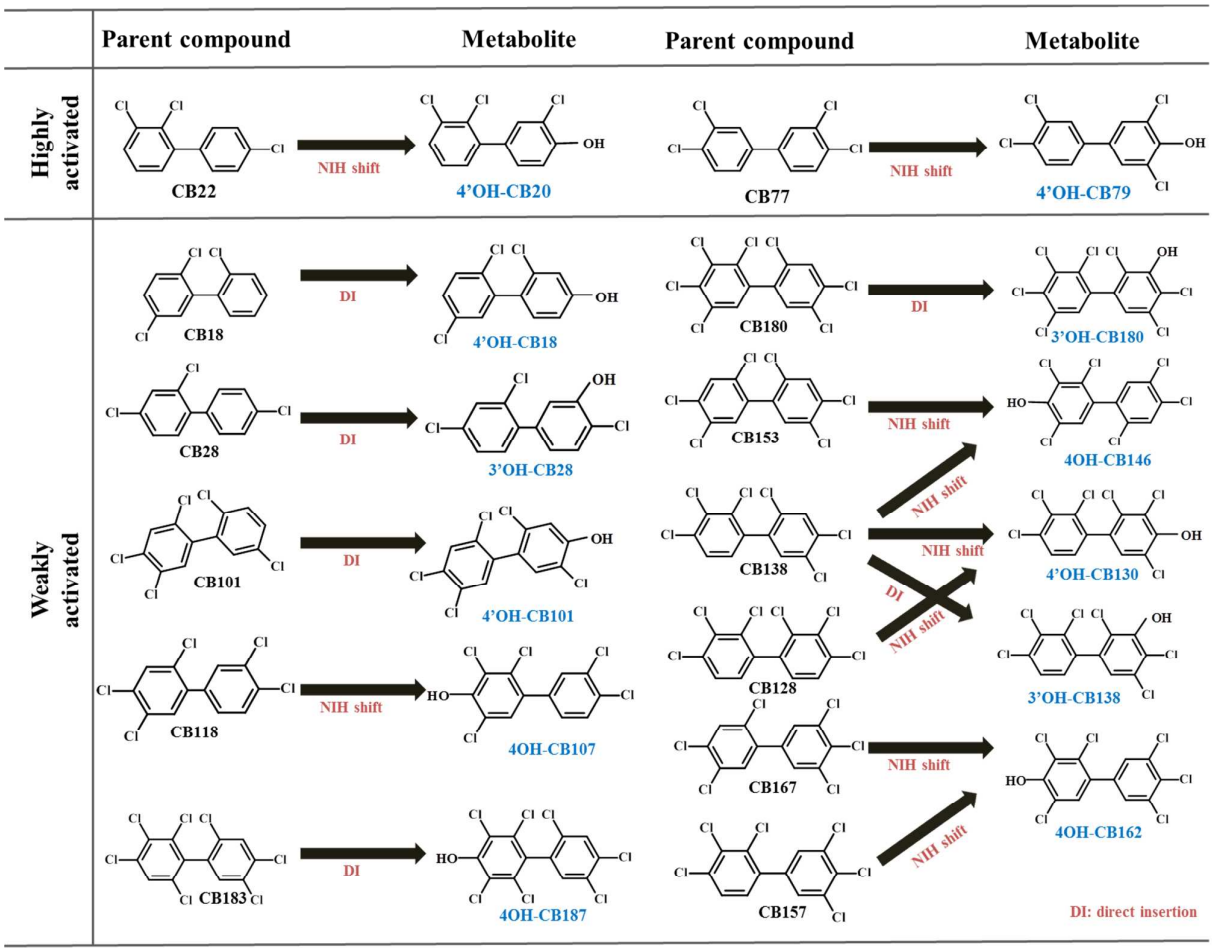

314

315 Figure S2.

316

(A)

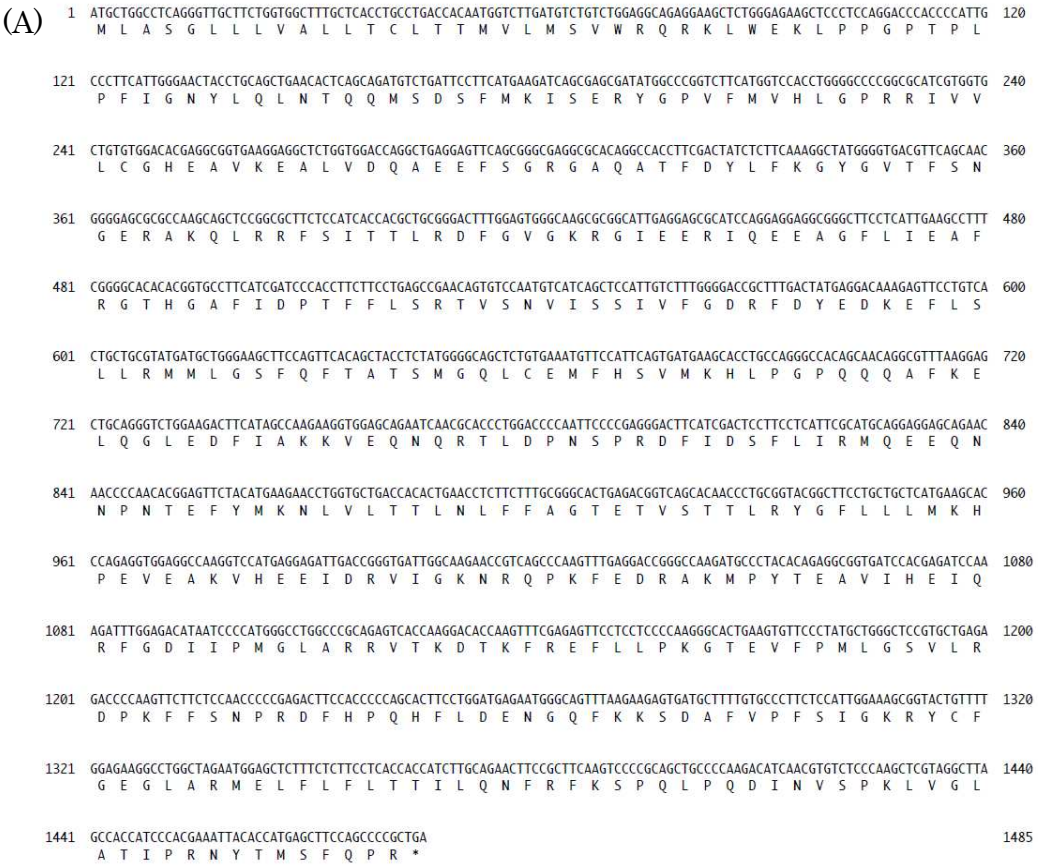

(B)

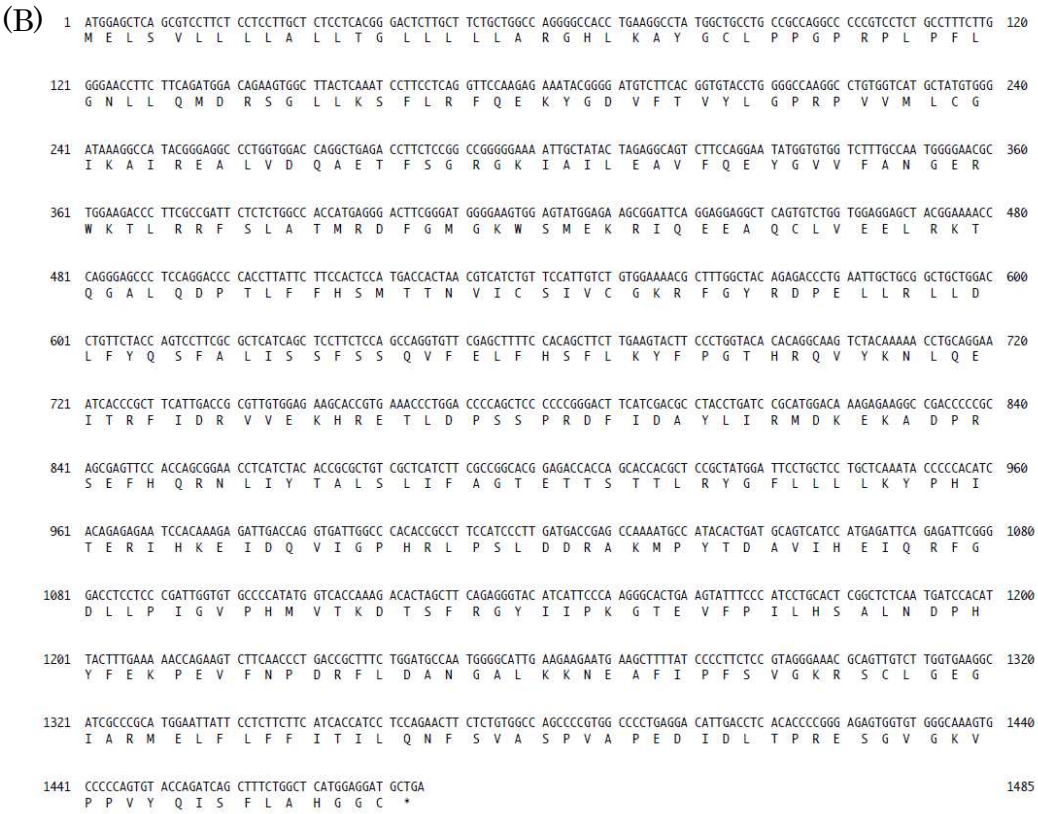

317 (continued)

(C)

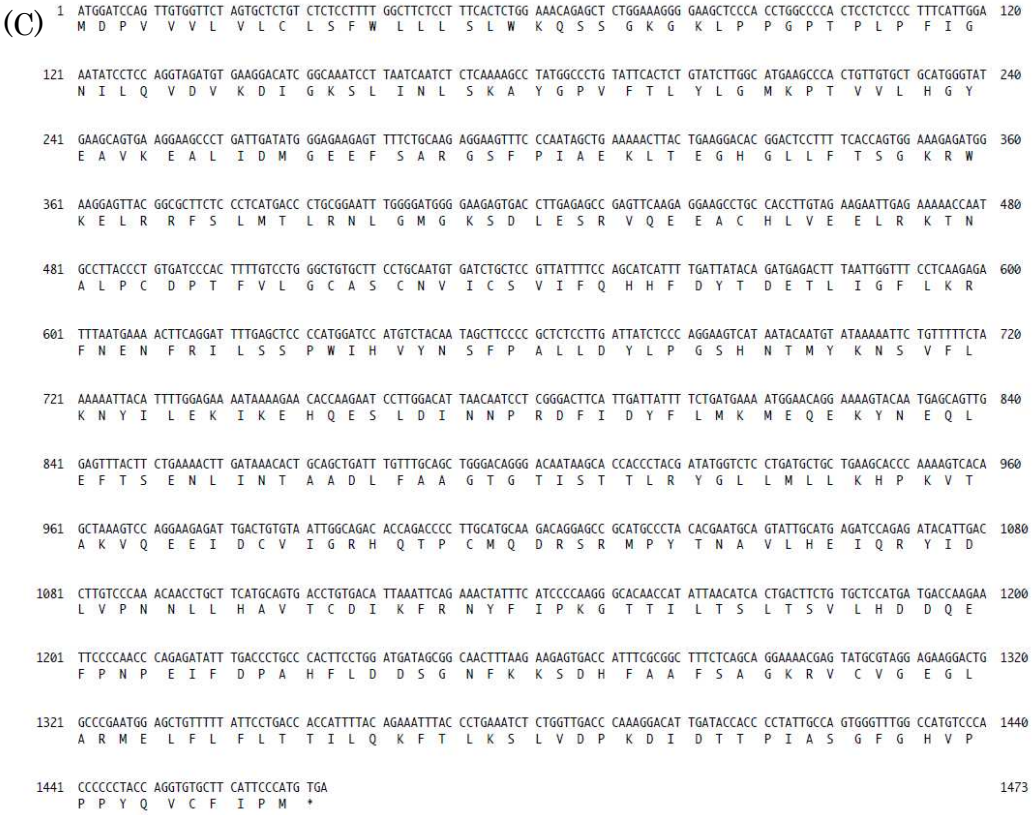
1 ATGGATCCAG TTGTGGTTCT AGTGCTCTGT CTCTCCTTTT GGCTTCTCCT TTCACTCTGG AAACAGAGCT CTGGAAAGGG GAAGCTCCCA CCTGGCCCCA CTCCTCTCCC TTTCATTGGA 120
M D P V V V L V L C L S F W L L L S L W K Q S S G K G K L P P G P T P L P F I G
121 AATATCCTCC AGGTAGATGT GAAGGACATC GGCAAATCCT TAATCAATCT CTCAAAAGCC TATGGCCCTG TATTCACTCT GTATCTTGGC ATGAAGCCCA CTGTTGTGCT GCATGGGTAT 240
N I L Q V D V K D I G K S L I N L S K A Y G P V F T L Y L G M K P T V V L H G Y
241 GAAGCAGTGA AGGAAGCCCT GATTGATATG GGAGAAGAGT TTTCTGCAAG AGGAAGTTTC CCAATAGCTG AAAAACTTAC TGAAGGACAC GGACTCCTTT TCACCAGTGG AAAGAGATGG 360
E A V K E A L I D M G E E F S A R G S F P I A E K L T E G H G L L F T S G K R W
361 AAGGAGTTAC GGCGCTTCTC CCTCATGACC CTGCGGAATT TGGGGATGGG GAAGAGTGAC CTTGAGAGCC GAGTTCAAGA GGAAGCCTGC CACCTTGTAG AAGAATTGAG AAAAACCAAT 480
K E L R R F S L M T L R N L G M G K S D L E S R V Q E E A C H L V E E L R K T N
481 GCCTTACCCT GTGATCCCAC TTTTGTCCTG GGCTGTGCTT CCTGCAATGT GATCTGCTCC GTTATTTTCC AGCATCATTT TGATTATACA GATGAGACTT TAATTGGTTT CCTCAAGAGA 600
A L P C D P T F V L G C A S C N V I C S V I F Q H H F D Y T D E T L I G F L K R
601 TTTAATGAAA ACTTCAGGAT TTTGAGCTCC CCATGGATCC ATGTCTACAA TAGCTTCCCC GCTCTCCTTG ATTATCTCCC AGGAAGTCAT AATACAATGT ATAAAAATTC TGTTTTTCTA 720
F N E N F R I L S S P W I H V Y N S F P A L L D Y L P G S H N T M Y K N S V F L
721 AAAAATTACA TTTTGGAGAA AATAAAAGAA CACCAAGAAT CCTTGGACAT TAACAATCCT CGGGACTTCA TTGATTATTT TCTGATGAAA ATGGAACAGG AAAAGTACAA TGAGCAGTTG 840
K N Y I L E K I K E H Q E S L D I N N P R D F I D Y F L M K M E Q E K Y N E Q L
841 GAGTTTACTT CTGAAAACTT GATAAACACT GCAGCTGATT TGTTTGCAGC TGGGACAGGG ACAATAAGCA CCACCCTACG ATATGGTCTC CTGATGCTGC TGAAGCACCC AAAAGTCACA 960
E F T S E N L I N T A A D L F A A G T G T I S T T L R Y G L L M L L K H P K V T
961 GCTAAAGTCC AGGAAGAGAT TGACTGTGTA ATTGGCAGAC ACCAGACCCC TTGCATGCAA GACAGGAGCC GCATGCCCTA CACGAATGCA GTATTGCATG AGATCCAGAG ATACATTGAC 1080
A K V Q E E I D C V I G R H Q T P C M Q D R S R M P Y T N A V L H E I Q R Y I D
1081 CTTGTCCCAA ACAACCTGCT TCATGCAGTG ACCTGTGACA TTAAATTCAG AAACTATTTC ATCCCCAAGG GCACAACCAT ATTAACATCA CTGACTTCTG TGCTCCATGA TGACCAAGAA 1200
L V P N N L L H A V T C D I K F R N Y F I P K G T T I L T S L T S V L H D D Q E
1201 TTCCCCAACC CAGAGATATT TGACCCTGCC CACTTCCTGG ATGATAGCGG CAACTTTAAG AAGAGTGACC ATTTCGCGGC TTTCTCAGCA GGAAAACGAG TATGCGTAGG AGAAGGACTG 1320
F P N P E I F D P A H F L D D S G N F K K S D H F A A F S A G K R V C V G E G L
1321 GCCCGAATGG AGCTGTTTTT ATTCCTGACC ACCATTTTAC AGAAATTTAC CCTGAAATCT CTGGTTGACC CAAAGGACAT TGATACCACC CCTATTGCCA GTGGGTTTGG CCATGTCCCA 1440
A R M E L F L F L T T I L Q K F T L K S L V D P K D I D T T P I A S G F G H V P
1441 CCCCCCTACC AGGTGTGCTT CATTCCCATG TGA 1473
P P Y Q V C F I P M *

Figure S3.

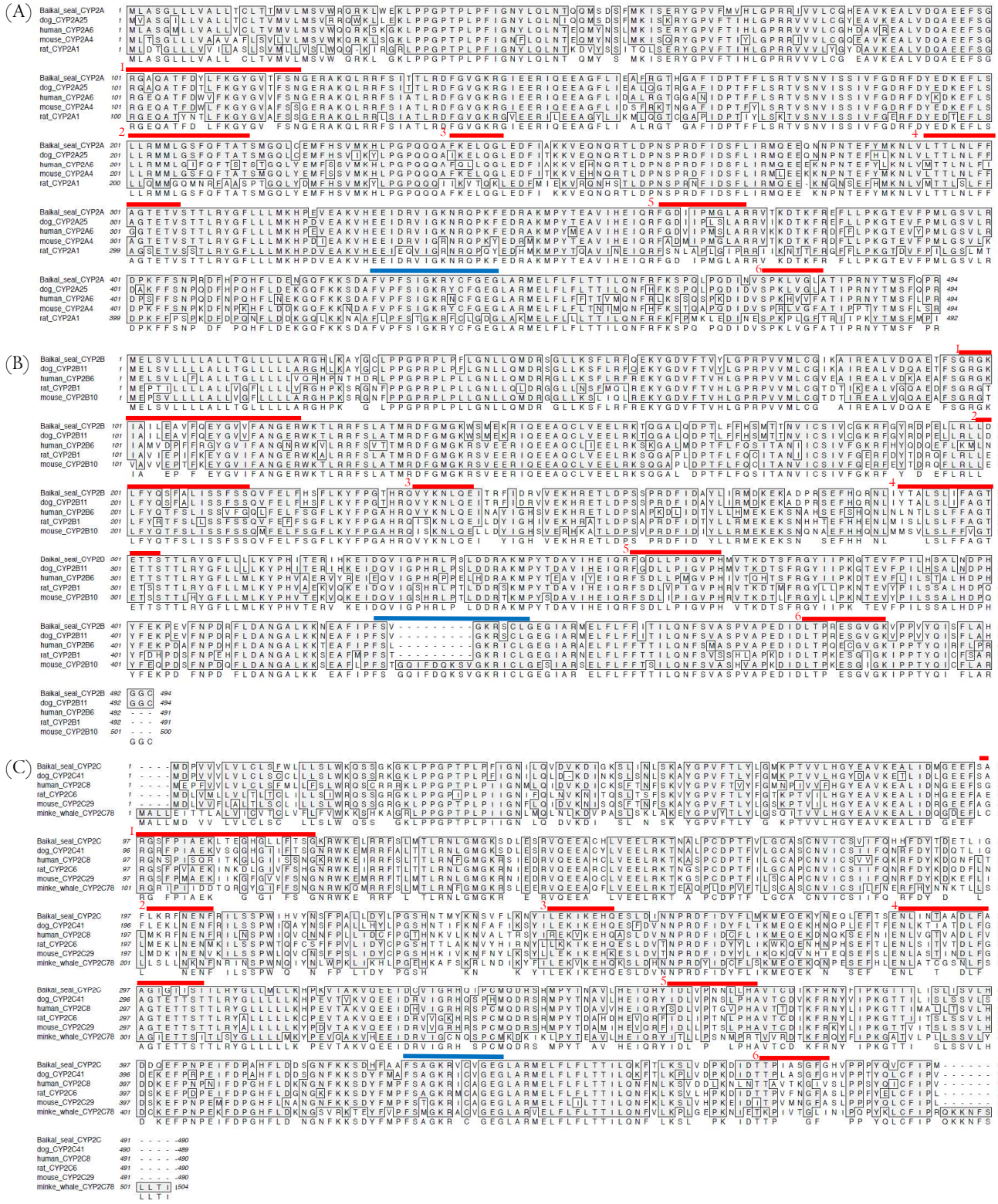

322 Figure S4.

323

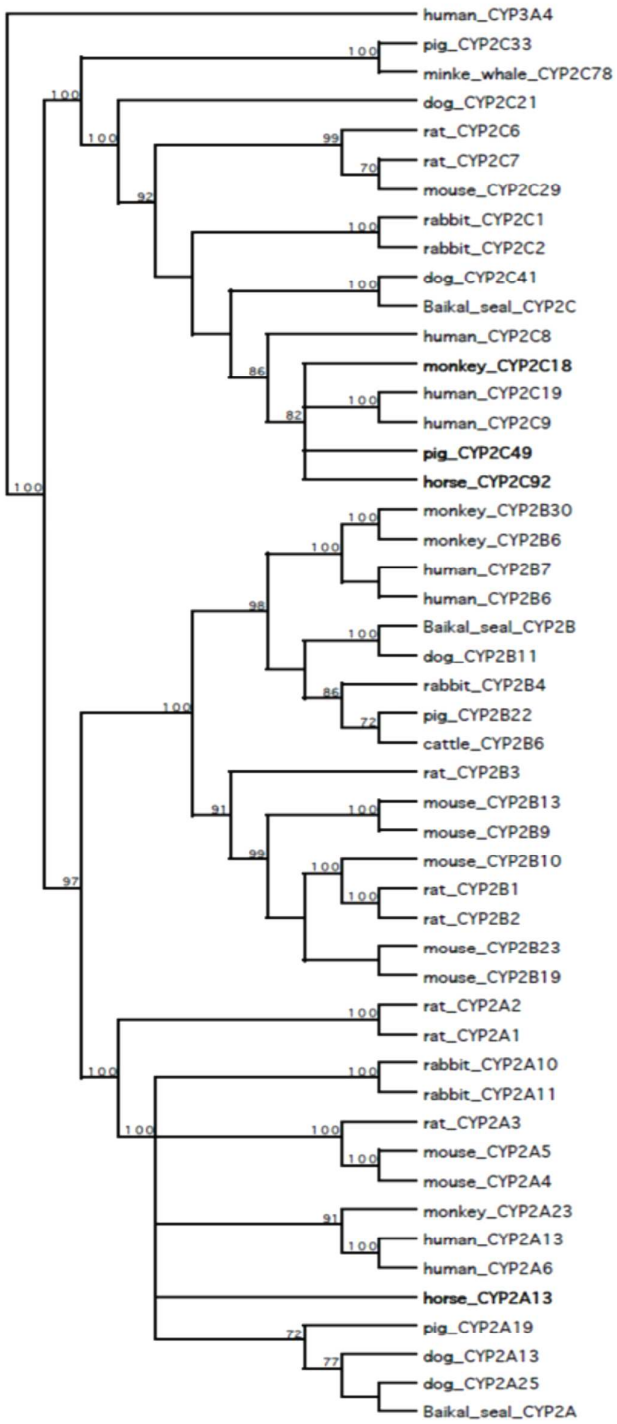
human_CYP3A4
pig_CYP2C33
minke_whale_CYP2C78
dog_CYP2C21
rat_CYP2C6
rat_CYP2C7
mouse_CYP2C29
rabbit_CYP2C1
rabbit_CYP2C2
dog_CYP2C41
Baikal_seal_CYP2C
human_CYP2C8
monkey_CYP2C18
human_CYP2C19
human_CYP2C9
pig_CYP2C49
horse_CYP2C92
monkey_CYP2B30
monkey_CYP2B6
human_CYP2B7
human_CYP2B6
Baikal_seal_CYP2B
dog_CYP2B11
rabbit_CYP2B4
pig_CYP2B22
cattle_CYP2B6
rat_CYP2B3
mouse_CYP2B13
mouse_CYP2B9
mouse_CYP2B10
rat_CYP2B1
rat_CYP2B2
mouse_CYP2B23
mouse_CYP2B19
rat_CYP2A2
rat_CYP2A1
rabbit_CYP2A10
rabbit_CYP2A11
rat_CYP2A3
mouse_CYP2A5
mouse_CYP2A4
monkey_CYP2A23
human_CYP2A13
human_CYP2A6
horse_CYP2A13
pig_CYP2A19
dog_CYP2A13
dog_CYP2A25
Baikal_seal_CYP2A

Figure S5.

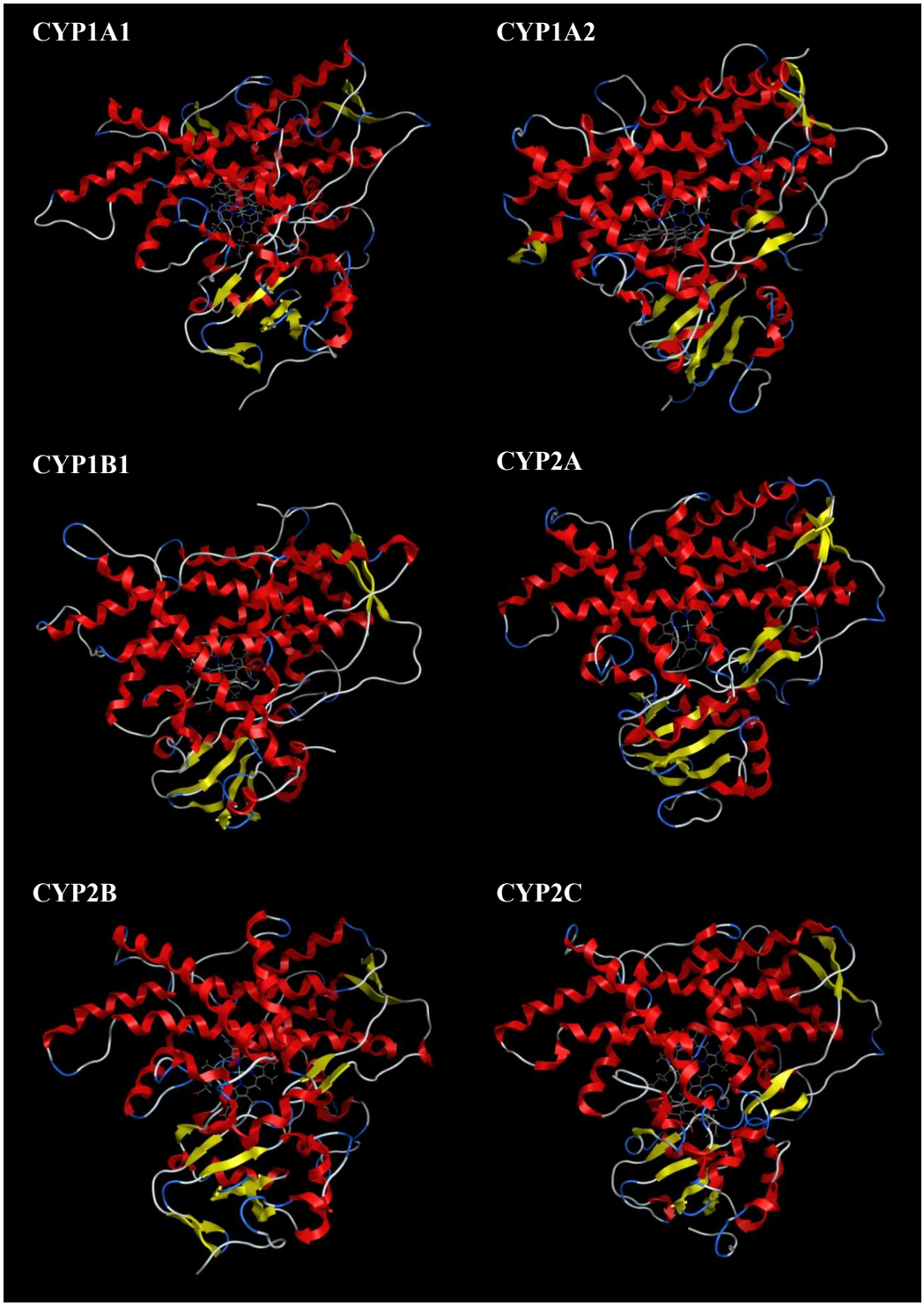

Figure S6.

329

330 (continued)

331

```
hCYP2C9   323 VQEEIERVIGRNRSPCMQDRSHMPYTDAVVHEVQRYIDLLPTSLPHAVTCDIKFRNYLIP 382
bsCYP1A1  347 IQEELDTVIGRARQPRLSDRPQLPYLEAFILETFRHASFVPFTIPHSTTKDTSLSGFYIP 406
bsCYP1A2  339 IQEELDTVTGRARQPRLSDRPQLPYMEAFILEVFRHTSFVPFTIPHSTTRDTTLKGFYIP 398
bsCYP1B1  356 VQAELDQVVGRDRLPCLDDQPNLPYVVAFLYEAMRFSSFVPVTIPHATTTSTSVLGYHIP 415
bsCYP2A   327 VHEEIDRVIGKNRQPKFEDRAKMPYTEAVIHEIQRFGDIIPMGLARRVTKDTKFREFLLP 386
bsCYP2B   324 IHKEIDQVIGPHRLPSLDDRAKMPYTDAVIHEIQRFGDLLPIGVPHMVTKDTSFRGYIIP 383
bsCYP2C   323 VQEEIDCVIGRHQTPCMQDRSRMPYTNAVLHEIQRYIDLVPNNLLHAVTCDIKFRNYFIP 382

hCYP2C9   383 KGTTILISLTSVLHDNKEFPNPEMFDPHHFLDEGGN---FKKSKYFMPFSAGKRICVGEA 439
bsCYP1A1  407 KGRCVFVNQWQINHDQELWGDPSEFRPERFLTLDGT-INKALSEKVILFGMGKRKCIGET 465
bsCYP1A2  399 KERCVFINQWHVNHDQKVWGDPFEFRPERFLTADGTSINKILSEKVMIFGMGKRRCIGEL 458
bsCYP1B1  416 KDTVVFVNQWSVNHDPAKWPNPEDFDPGRFLDKDGC-IDKDLASSVMIFSMGKRRCIGEE 474
bsCYP2A   387 KGTEVFPMLGSVLRDPKFFSNPRDFHPQHFLDENGQ---FKKSDAFVPFSIGKRYCFGEG 443
bsCYP2B   384 KGTEVFPILHSALNDPHYFEKPEVFNPDRFLDANGA---LKKNEAFIPFSVGKRSCLGEG 440
bsCYP2C   383 KGTTILTSLTSVLHDDQEFPNPEIFDPAHFLDDSGN---FKKSDHFAAFSAGKRVCVGEG 439

hCYP2C9   440 LAGMELFLFLTSILQNFNLKSLVDPKNLDTTPVVNGFASVPPFYQLCFIPV--------- 490
bsCYP1A1  466 IARLEVFLFLAILLQQVEFSVPRG-TKVDMTPIYGLTMKHARCEHVQVRVRA-------- 516
bsCYP1A2  459 LAKWEIFLFLAILLQRLEFSVPDG-VKVDLTPIYGLIMKHTRCEHVQARPRFSTK----- 512
bsCYP1B1  475 LSKMQLFLFISILAHECNFKANPD--EPSKMDFNYGLTIKPKSFRINVTLRESMELLDSA 532
bsCYP2A   444 LARMELFLFLTTILQNFRFKSPQLPQDINVSPKLVGLATIPRNYTMSFQPR--------- 494
bsCYP2B   441 IARMELFLFFITILQNFSVASPVAPEDIDLTPRESGVGKVPPVYQISFLAHGGC------ 494
bsCYP2C   440 LARMELFLFLTTILQKFTLKSLVDPKDIDTTPIASGFGHVPPPYQVCFIPM--------- 490

hCYP2C9   491 ---------- 490
bsCYP1A1  517 ---------- 516
bsCYP1A2  513 ---------- 512
bsCYP1B1  533 VQKFQAEEDCQ 543
bsCYP2A   495 ---------- 494
bsCYP2B   495 ---------- 494
bsCYP2C   491 ---------- 490
```

Figure S7.

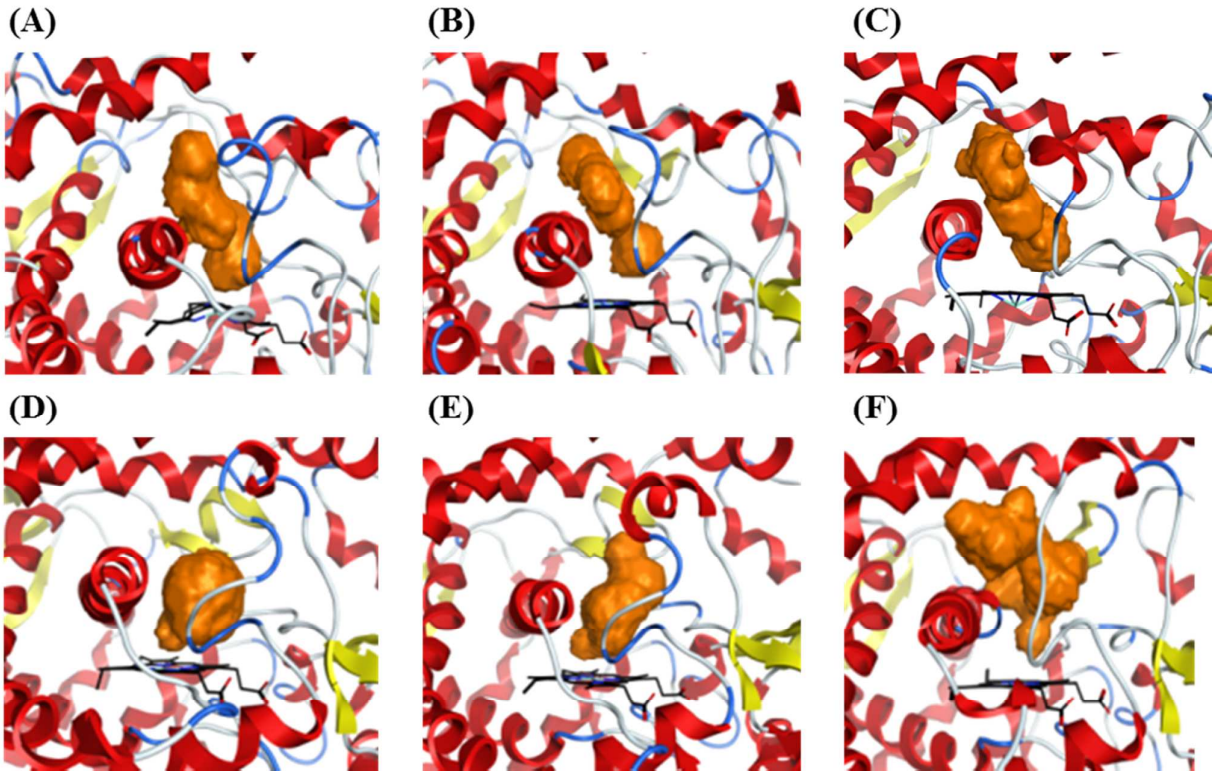

Figure S8.

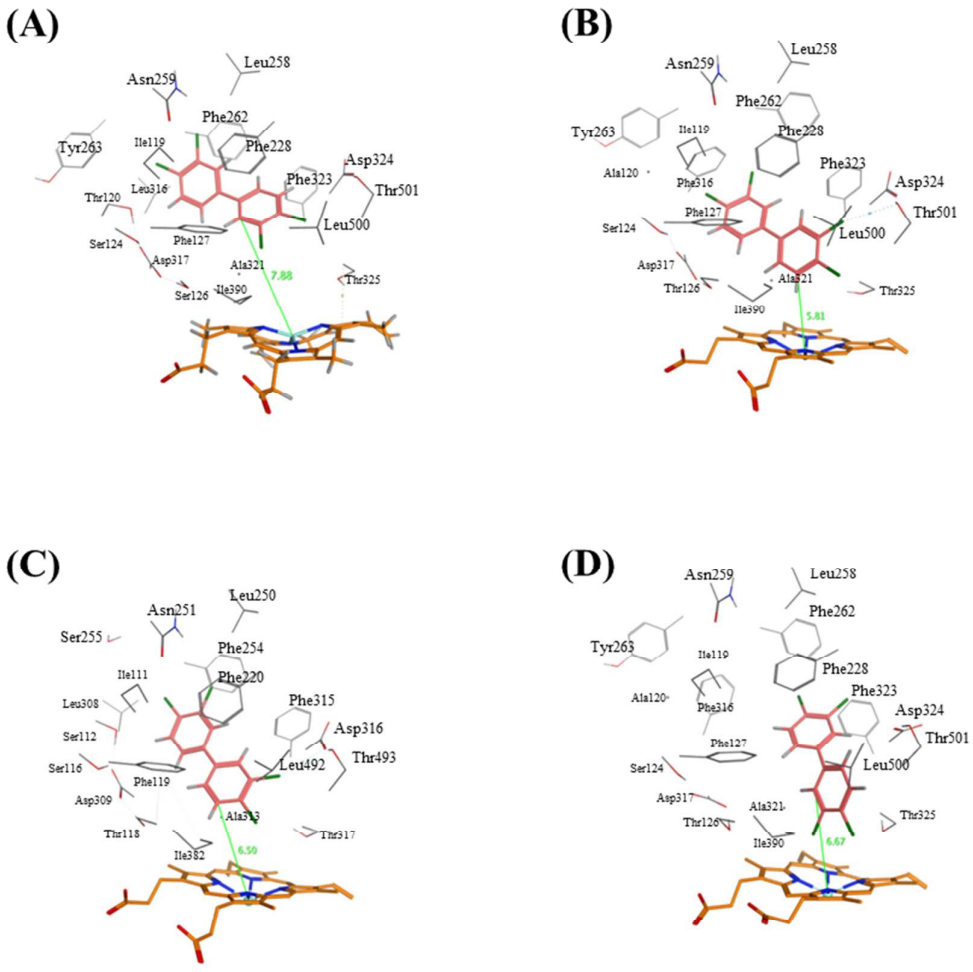
(A)
Asn259
Leu258
Phe262
Tyr263
Ile119
Phe228
Asp324
Phe323
Thr501
Thr120
Leu316
Leu500
Ser124
Phe127
Asp317
Ala321
7.88
Ser126
Ile390
Thr325
(B)
Asn259
Leu258
Phe262
Tyr263
Ile119
Phe228
Ala120
Phe323
Asp324
Phe316
Thr501
Phe127
Ser124
Leu500
Asp317
Thr126
Ala321
Thr325
Ile390
5.81
(C)
Asn251
Leu250
Ser255
Phe254
Phe220
Ile111
Phe315
Leu308
Asp316
Ser112
Thr493
Ser116
Leu492
Phe119
Asp309
Ala313
Thr118
Thr317
Ile382
6.50
(D)
Asn259
Leu258
Phe262
Tyr263
Ile119
Phe228
Ala120
Phe323
Asp324
Phe316
Thr501
Phe127
Ser124
Leu500
Asp317
Ala321
Thr126
Thr325
Ile390
6.67

Figure S9.

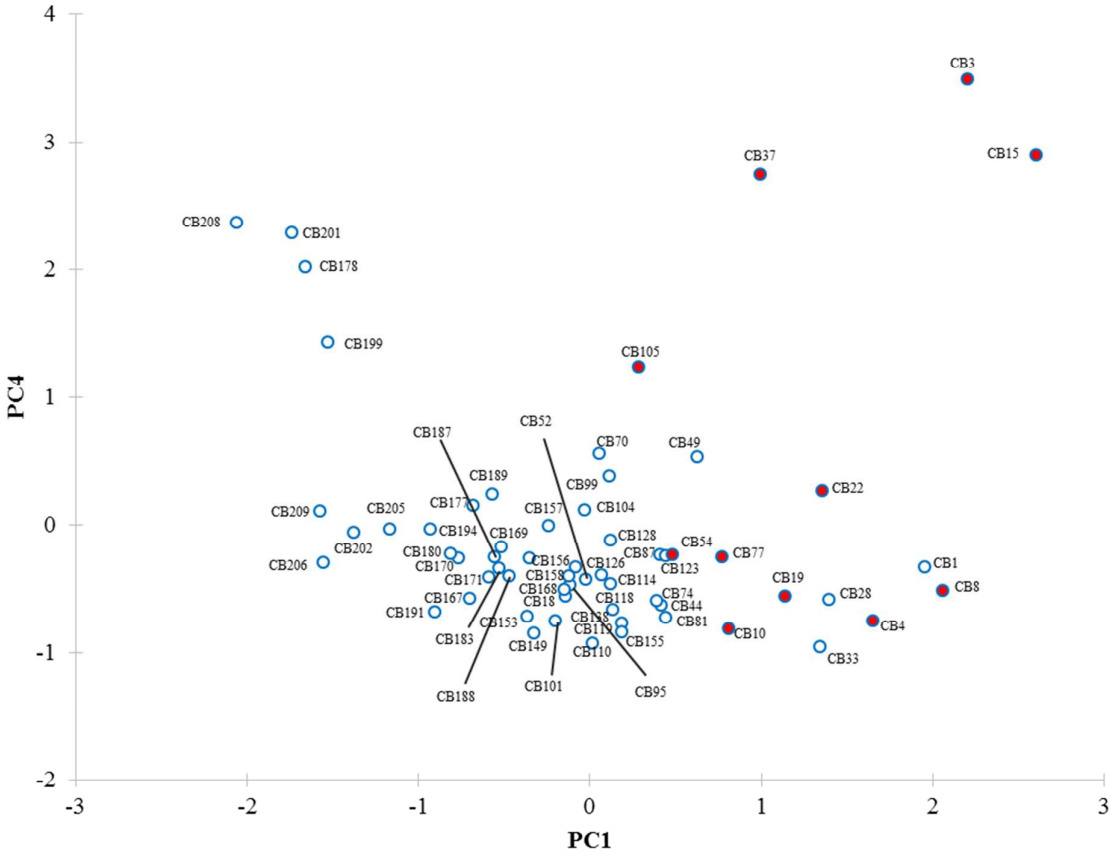
PC4
PC1
4
3
2
1
0
-1
-2
-3
-2
-1
0
1
2
3
CB3
CB37
CB15
CB208
CB201
CB178
CB199
CB105
CB52
CB187
CB70
CB49
CB189
CB99
CB22
CB209
CB205
CB177
CB157
CB104
CB194
CB169
CB128
CB54
CB202
CB180
CB156
CB87
CB77
CB206
CB170
CB126
CB123
CB1
CB171
CB158
CB114
CB19
CB8
CB167
CB168
CB74
CB28
CB191
CB18
CB118
CB44
CB153
CB81
CB4
CB183
CB149
CB110
CB155
CB10
CB33
CB188
CB101
CB95

Figure S10.